Supporting Information

Durable and Self-Healing Superamphiphobic Coatings Repellent Even towards Hot Liquids

*Bucheng Li, and Junping Zhang**

Center of Eco-material and Green Chemistry, Lanzhou Institute of Chemical Physics, Chinese Academy of Sciences, Tianshui Middle Road 18, Lanzhou 730000 (P. R. China)

Fax: (+86) 931-8277088

E-mail: jpzhang@licp.cas.cn

Materials. TEOS (99.9%) and PFDTES (97%) were purchased from Sigma-Aldrich. PAL, supplied by Jiuchuan Technology Co. Ltd, Jiangsu, China, is composed of 1.29% CaO, 10.47% Al_2O_3, 1.52% Na_2O, 20.41% MgO, 64.31% SiO_2, 0.13% K_2O and 0.87% Fe_2O_3 as determined by X-ray fluorescence spectrometer (PANalytical Co., MiniPal 4). The price of PAL is ~2 ¥/kg, which is negligible compared to that of PFDTES. Anhydrous ethanol, ammonia (25-28 wt%), diiodomethane, *n*-hexadecane, *n*-dodecane, *n*-decane, *n*-octane and toluene were purchased from China National Medicines Co. Ltd. Halloysite was purchased from Sigma-Aldrich. Na^+-montmorillonite and sepiolite were purchased from Huanqiu Minerals, Dalian, China. Glass slides (Menzel, Braunschweig, Germany) were used as the main substrates for spray coating. Other reagents used were all of analytical grade. All chemicals were used as received without further purification.

Preparation of PAL@fluoroPOS Suspensions. The PAL@fluoroPOS suspensions were prepared by a modified Stöber method.[1] In a typical synthesis, 0.5 g of PAL was dispersed in a solution containing 40 mL of anhydrous ethanol and 10 mL of ammonia aqueous solution. The suspension was ultrasonicated for 30 min, and then proper amounts of TEOS and PFDTES were injected quickly into the suspension under vigorous stirring at 800 rpm. After reacting at room conditions for 6 h, the homogeneous PAL@fluoroPOS suspensions were formed. Other clay minerals such as sepiolite, halloysite and

Na^+-montmorillonite were also used to prepare the suspensions instead of PAL according to the same procedure.

Preparation of Superamphiphobic PAL@fluoroPOS/PFDTES Coatings. First, the glass slides were ultrasonicated for 1 h in a 10% v/v solution of Techogent T105 at 50 ℃, rinsed with deionized water, and dried under a N_2 flow. The spray-coating suspension was prepared by adding a proper amount of PFDTES into 4 mL of the as-prepared PAL@fluoroPOS suspension. The spray-coating suspension was magnetically stirred for 5 min, and then spray-coated onto the vertically placed glass slide using an airbrush (INFINITY 2 in 1, Harder & Steenbeck, Germany) with 0.2 MPa N_2 at a distance of 15 cm. The glass slide was attached on a hot plate with a temperature of 90 ℃ to accelerate the evaporation of ethanol in the spray-coating process. Other materials including polyurethane plate, wood plate, polyester textile, PTFE plate and aluminium plate were also used as substrates for spray-coating instead of the glass slide. All of the substrates were cleaned by washing in turn with ethanol, acetone and distilled water, and then dried under a N_2 flow.

Mechanical, Environmental and Chemical Durability Tests. The mechanical, environmental and chemical durability of the coatings was investigated via various approaches including water jetting tests, peeling with adhesive tape and finger press. For the water jetting tests, water jet at certain pressure scoured the 45 ° tilted coating from a height of 20 cm for a period of time (Fig. S16). Durability of the coatings against UV irradiation, harsh temperatures, corrosive liquids, organic solvents and boiling liquids were also studied. After all the durability tests, the $CA_{n\text{-decane}}$ and $SA_{n\text{-decane}}$ on the samples were measured to evaluate their superamphiphobicity.

Self-Healing Ability Test. To demonstrate the self-healing ability, the PAL@fluoroPOS/PFDTES coating was damaged artificially by air plasma for 5 min. The damaged coating was placed at room conditions for 24 h to accomplish the self-healing process. The plasma/self-healing tests were repeated for five times, and the changes in the $CA_{n\text{-decane}}$ and $SA_{n\text{-decane}}$ were recorded.

Measurements of CAs and SAs. Measurements of CAs and SAs were performed with a Contact Angle System OCA20 (Dataphysics, Germany) equipped with a tilting table. The

syringe was positioned in a way that the liquid droplets (5 μL) could contact surface of the samples before leaving the needle. Tilting angle of the table was adjustable (0 ~ 70 °) and allowed the subsequent measurement of the SAs at the same position on the sample. Because the temperature of liquid droplets decreases quickly, it is difficult to get the real temperature of hot liquid droplets on the coatings. The temperature of hot liquid droplets reported in this paper is the temperature of liquids in the syringe used for measurements of CAs and SAs. The temperature was measured by an IR sensor. In order to reduce thermal loss from the liquid droplets on the coatings, measurements of CAs and SAs were carried out within 5 s of placing the droplets on the coatings. A minimum of six readings were recorded for each sample, and the average values with standard errors were reported.

Characterization. FTIR spectra of samples were recorded on a Thermo Nicolet NEXUS TM spectrophotometer using KBr pellets. The micrographs of the samples were taken using a field emission scanning electron microscope (SEM, JSM-6701F, JEOL) and a field emission transmission electron microscope (TEM, JEM-1200EX, FEI). Before SEM observation, all samples were fixed on aluminum stubs and coated with gold (~ 7 nm). For TEM observation, the samples were prepared as follows. A drop of the suspension in was put on a copper grid and dried in the open atmosphere. The C, O, F and Si elemental maps in the samples were obtained using an energy dispersive spectrometer (EDS) of SEM. The XPS spectra of samples were obtained using a VG ESCALAB 250 Xi spectrometer equipped with a Monochromated Al Kα X-ray radiation source and a hemispherical electron analyzer. The spectra were recorded in the constant pass energy mode with a value of 100 eV, and all binding energies were calibrated using the C1s peak at 284.6 eV as the reference.

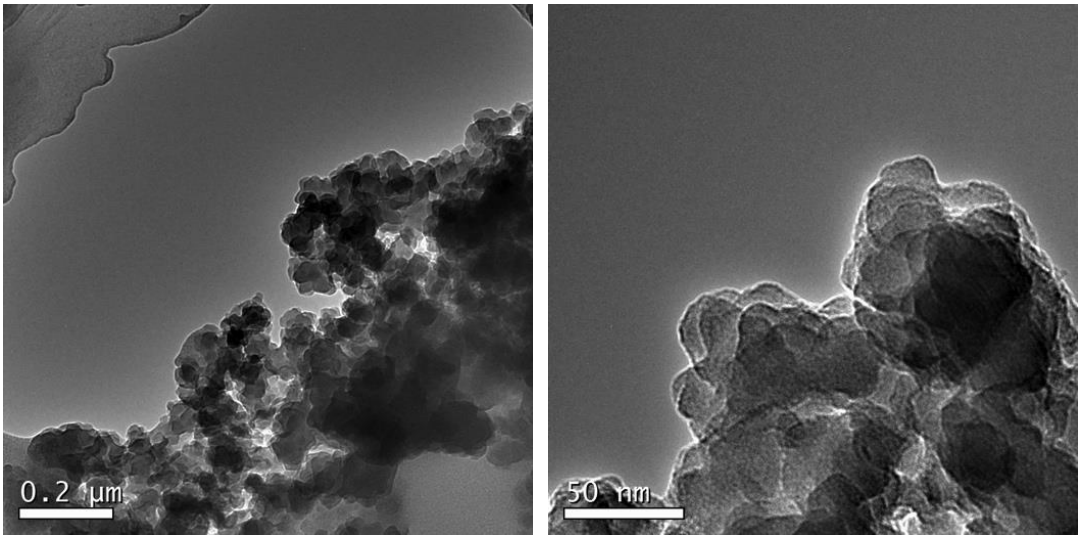

Fig. S1. TEM images of fluoroPOS prepared in the absence of PAL. $C_{PFDTES-i}$ = 25 mM and C_{TEOS} = 4.5 mM.

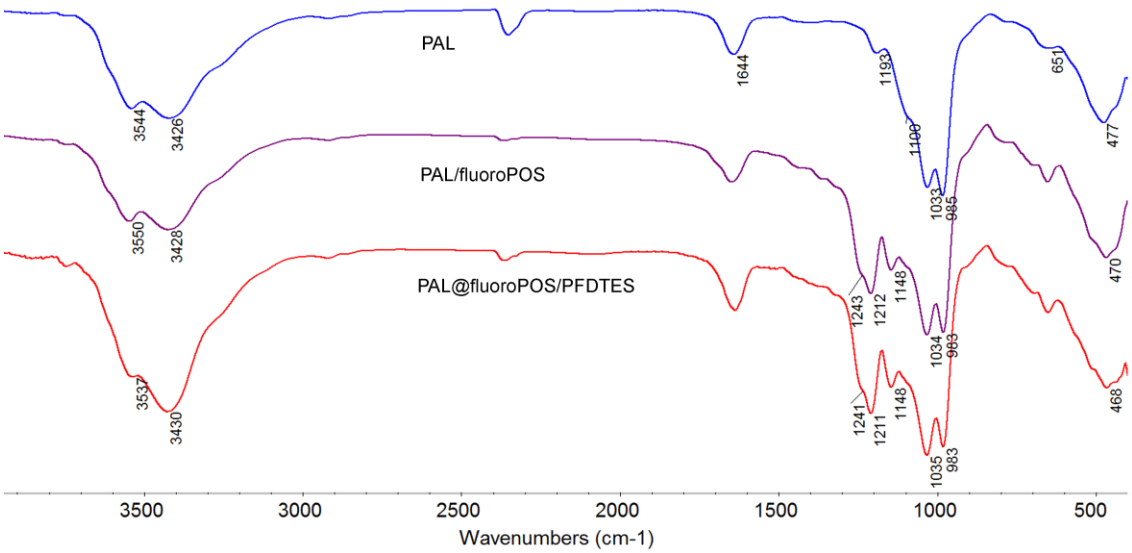

Fig. S2. FTIR spectra of PAL, PAL@fluoroPOS and PAL@fluoroPOS/PFDTES. C_{PAL} = 10 g L^{-1}, $C_{PFDTES-i}$ = 25 mM, C_{TEOS} = 4.5 mM and $C_{PFDTES-ii}$ = 11.3 mM.

After modification with PFDTES and TEOS, the C-F bands at 1241 and 1212 cm^{-1} were easily recognized in the spectrum of PAL@fluoroPOS.[2] The band at 1212 cm^{-1} was attributed to both the C-F group and the Si-O group (1193 cm^{-1}). The band at 1148 cm^{-1} was attributed to the possible silsesquioxane bands stemming from the co-condensation of hydrolyzed PFDTES and TEOS. In the spectrum of PAL@fluoroPOS/PFDTES, the $-OCH_2CH_3$ bands (956, 820 and 778 cm^{-1}) of PFDTES were not detected, suggesting complete hydrolysis of PFDTES. The Si-OH groups generated by hydrolysis of PFDTES could form additional crosslinking points with fluoroPOS.

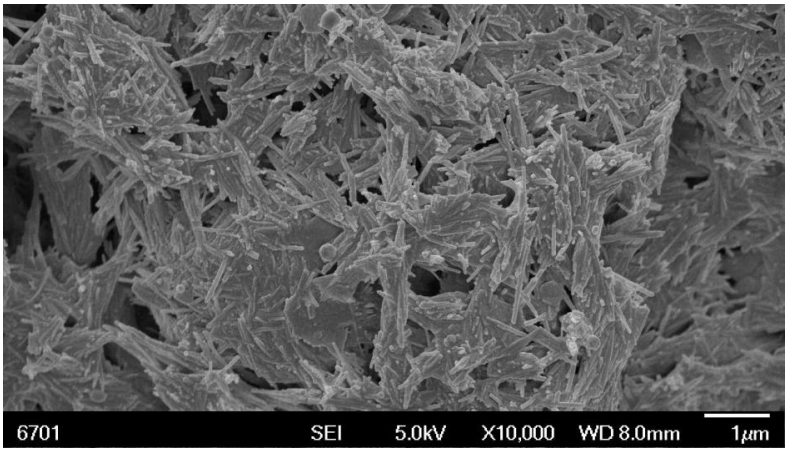

Fig. S3. SEM image of the PAL@fluoroPOS coating. C_{PAL} = 10 g L^{-1}, $C_{PFDTES-i}$ = 25 mM and C_{TEOS} = 4.5 mM.

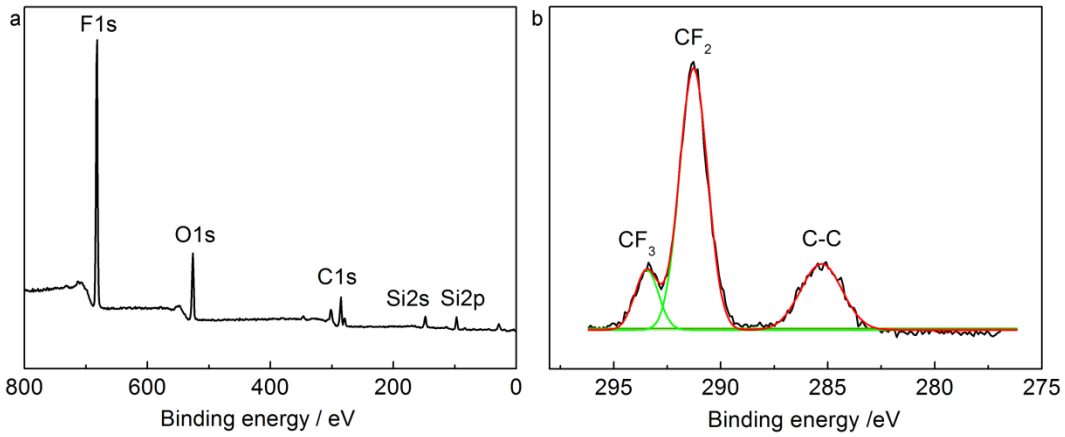

Fig. S4. (a) XPS survey spectrum and (b) C 1s spectrum of the PAL@fluoroPOS/PFDTES coating. C_{PAL} = 10 g L^{-1}, $C_{PFDTES-i}$ = 25 mM, C_{TEOS} = 4.5 mM and $C_{PFDTES-ii}$ = 11.3 mM.

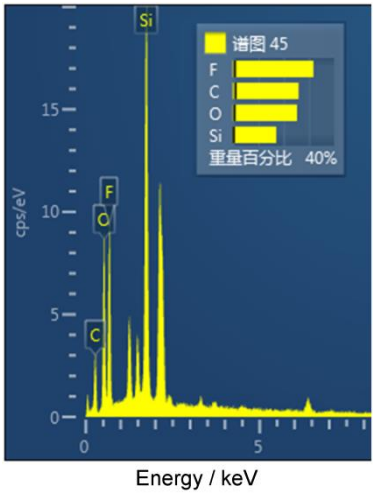

Fig. S5. EDS spectrum of the PAL@fluoroPOS/PFDTES coating. C_{PAL} = 10 g L^{-1}, $C_{PFDTES-i}$ = 25 mM, C_{TEOS} = 4.5 mM and $C_{PFDTES-ii}$ = 11.3 mM.

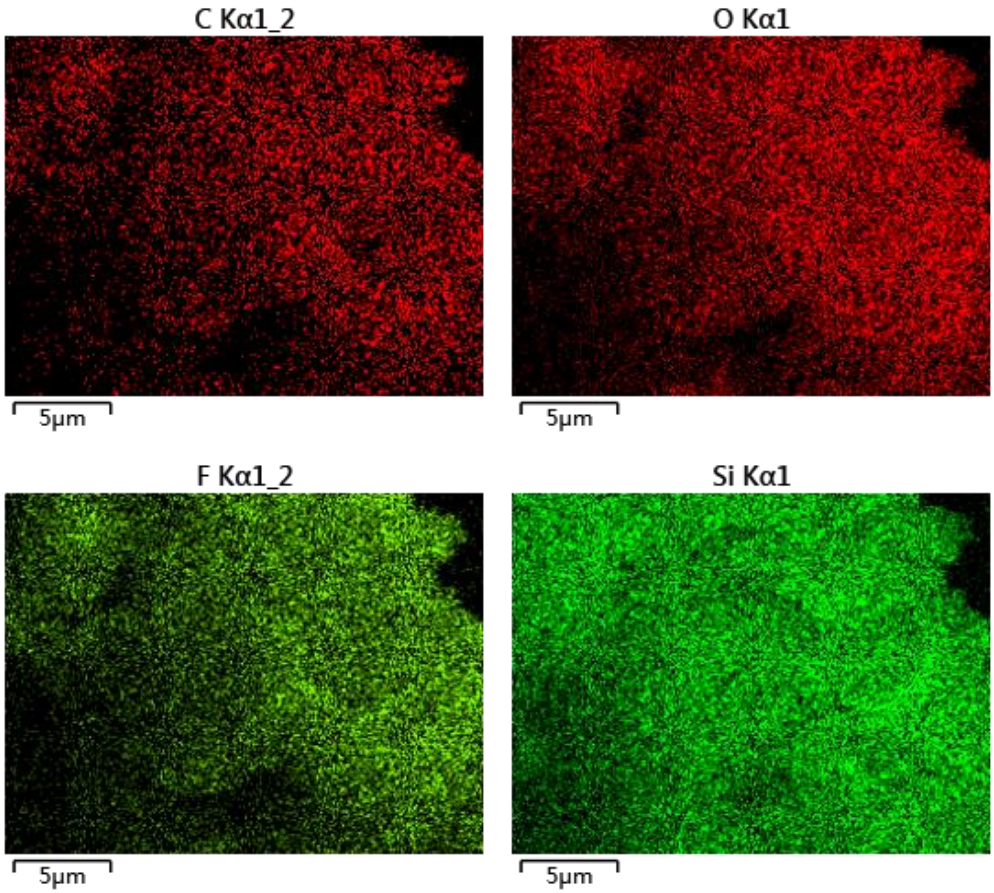

Fig. S6. EDS C, O, F and Si elemental maps of the PAL@fluoroPOS/PFDTES coating. C_{PAL} = 10 g L^{-1}, $C_{PFDTES\text{-}i}$ = 25 mM, C_{TEOS} = 4.5 mM and $C_{PFDTES\text{-}ii}$ = 11.3 mM.

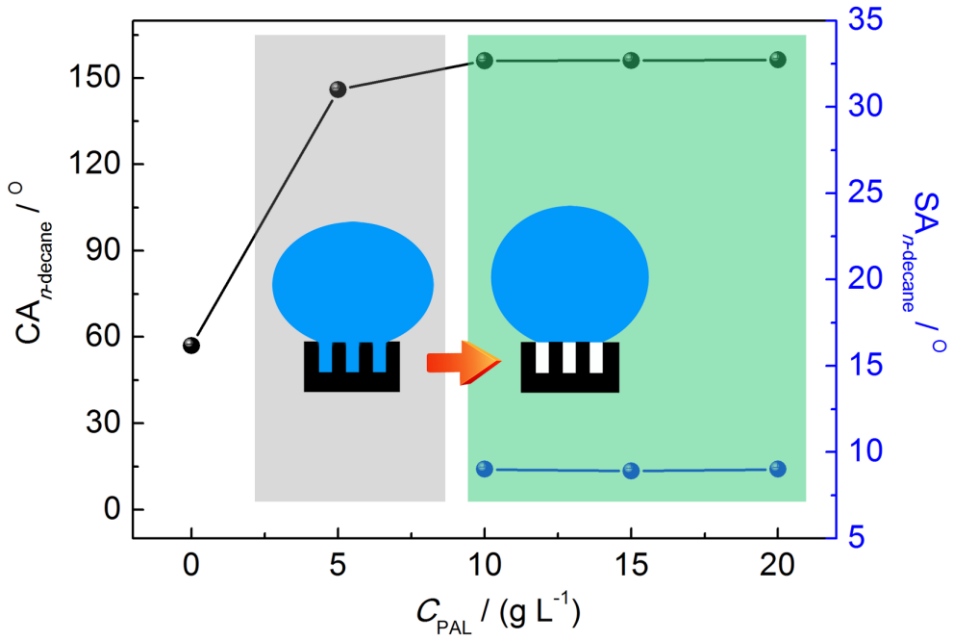

Fig. S7. Variation of $CA_{n\text{-decane}}$ and $SA_{n\text{-decane}}$ of the PAL@fluoroPOS coatings with C_{PAL}. $C_{PFDTES\text{-}i}$= 25 mM and C_{TEOS} = 4.5 mM.

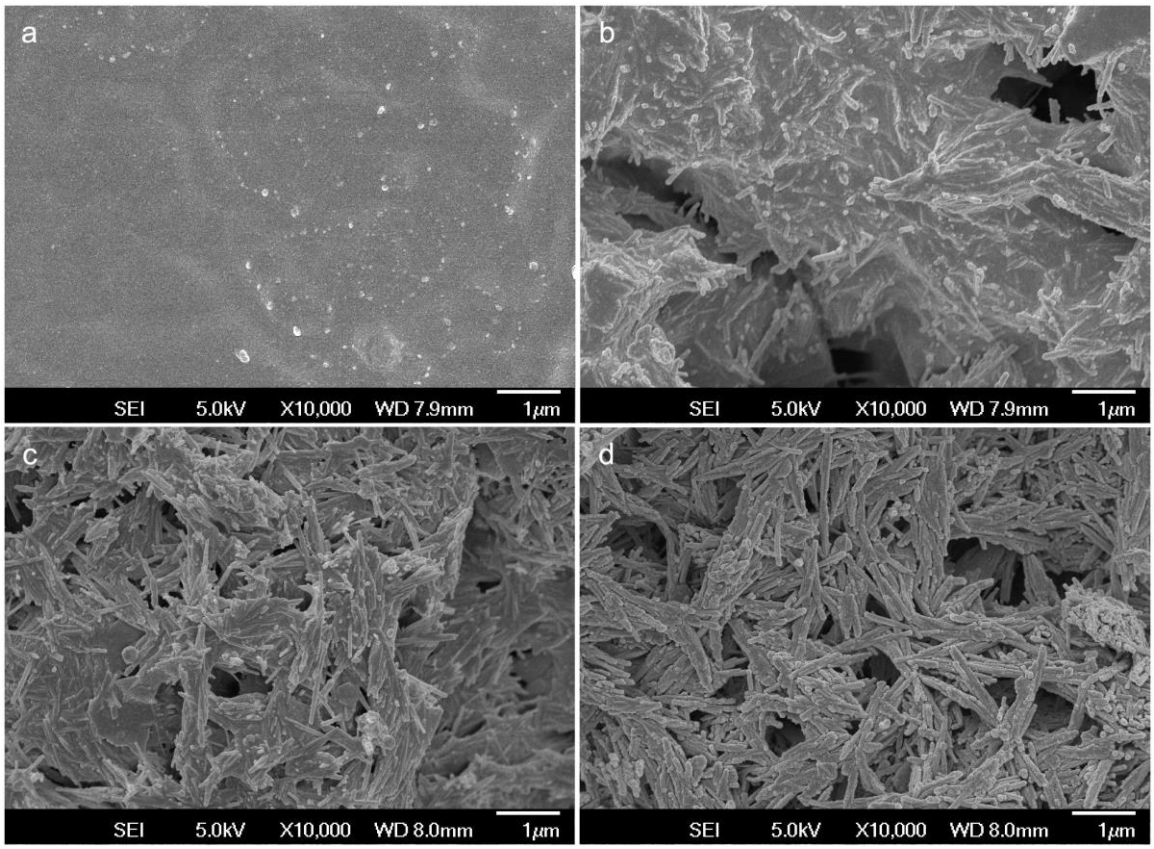

Fig. S8. SEM images of the PAL@fluoroPOS coatings with a C_{PAL} of (a) 0, (b) 5, (c) 10 and (d) 15 g L^{-1}. $C_{PFDTES\text{-}i}$ = 25 mM and C_{TEOS} = 4.5 mM.

Table S1. Effects of the kind of clay minerals on the $CA_{n\text{-octane}}$ and $SA_{n\text{-octane}}$ of the Clay@fluoroPOS coatings. C_{clay} = 10 g L^{-1}, $C_{PFDTES\text{-}i}$ = 25 mM and C_{TEOS} = 4.5 mM.

Clay minerals	$CA_{n\text{-octane}}$ / °	$SA_{n\text{-octane}}$ / °
PAL	152.7 ± 0.8	18.3 ± 1.2
sepiolite	151.2 ± 0.9	38.0 ± 2.6
halloysite	119.6 ± 1.8	-
Na^+-montmorillonite	128.3 ± 1.3	-

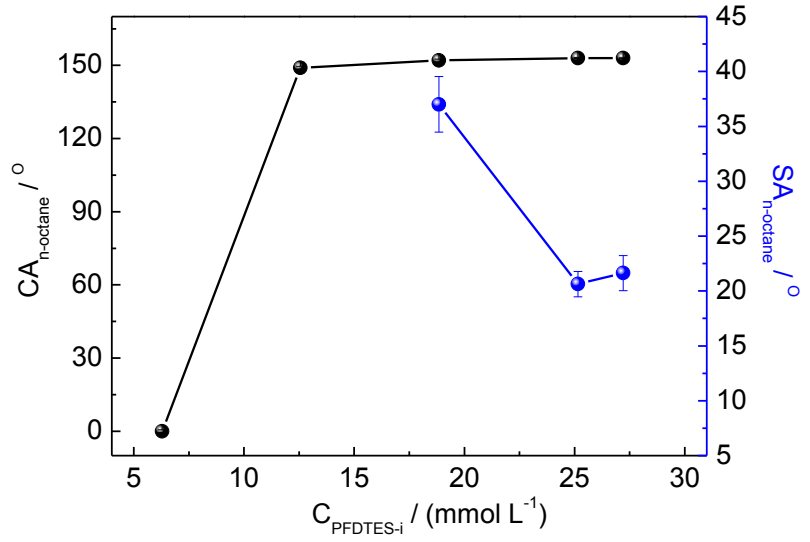

Fig. S9. Variation of $CA_{n\text{-octane}}$ and $SA_{n\text{-octane}}$ of the PAL@fluoroPOS coatings with $C_{PFDTES\text{-}i}$. C_{PAL}= 10 g L^{-1} and C_{TEOS} = 4.5 mM.

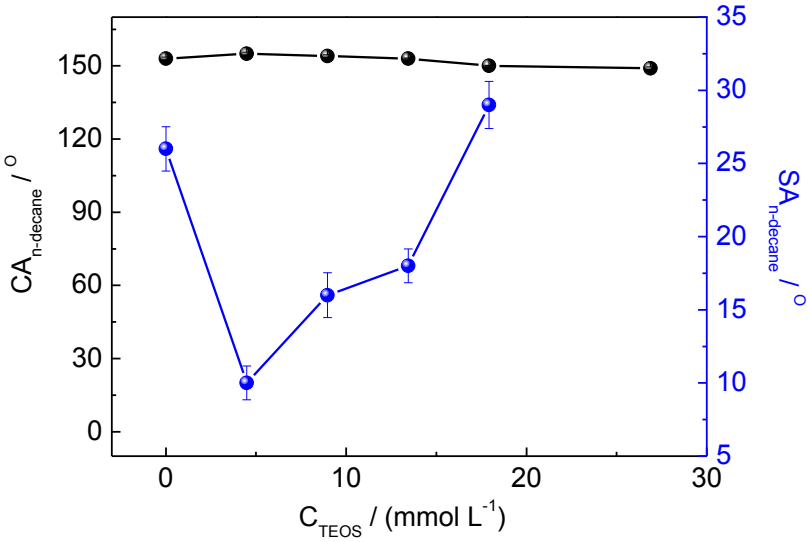

Fig. S10. Variation of $CA_{n\text{-decane}}$ and $SA_{n\text{-decane}}$ of the PAL@fluoroPOS coatings with C_{TEOS}. C_{PAL}= 10 g L^{-1} and $C_{PFDTES\text{-}i}$ = 25 mM.

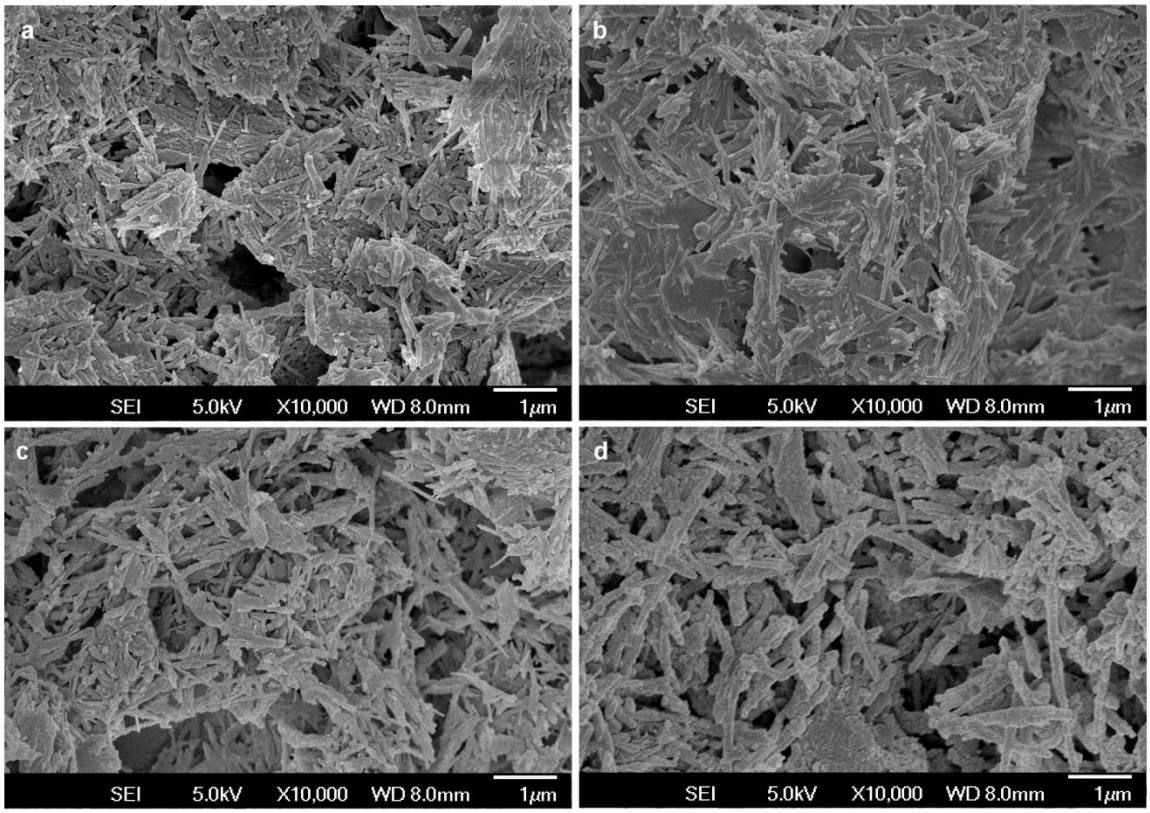

Fig. S11. SEM images of the PAL@fluoroPOS coatings with a C_{TEOS} of (a) 0, (b) 4.5, (c) 17.9 and (d) 26.9 mM. C_{PAL}= 10 g L^{-1} and $C_{PFDTES\text{-}i}$ = 25 mM.

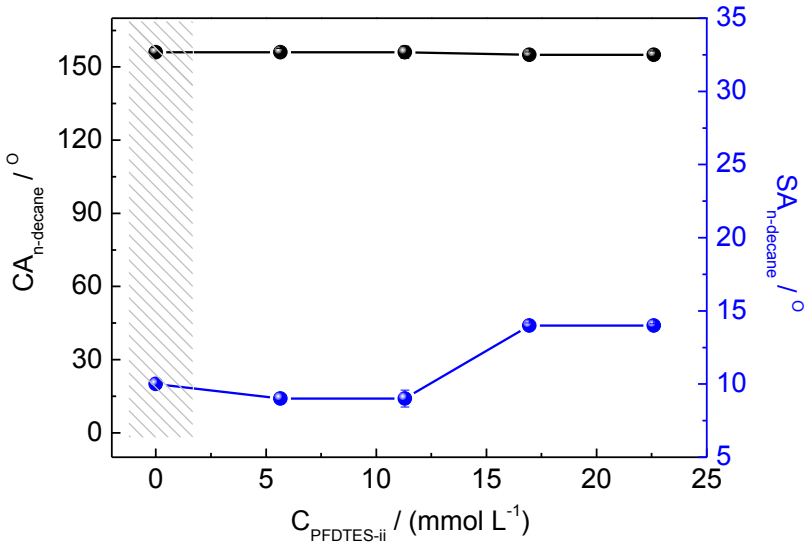

Fig. S12. Variation of $CA_{n\text{-decane}}$ and $SA_{n\text{-decane}}$ of the PAL@fluoroPOS/PFDTES coatings with $C_{PFDTES\text{-}ii}$. C_{PAL} = 10 g L^{-1}, $C_{PFDTES\text{-}i}$ = 25 mM and C_{TEOS} = 4.5 mM.

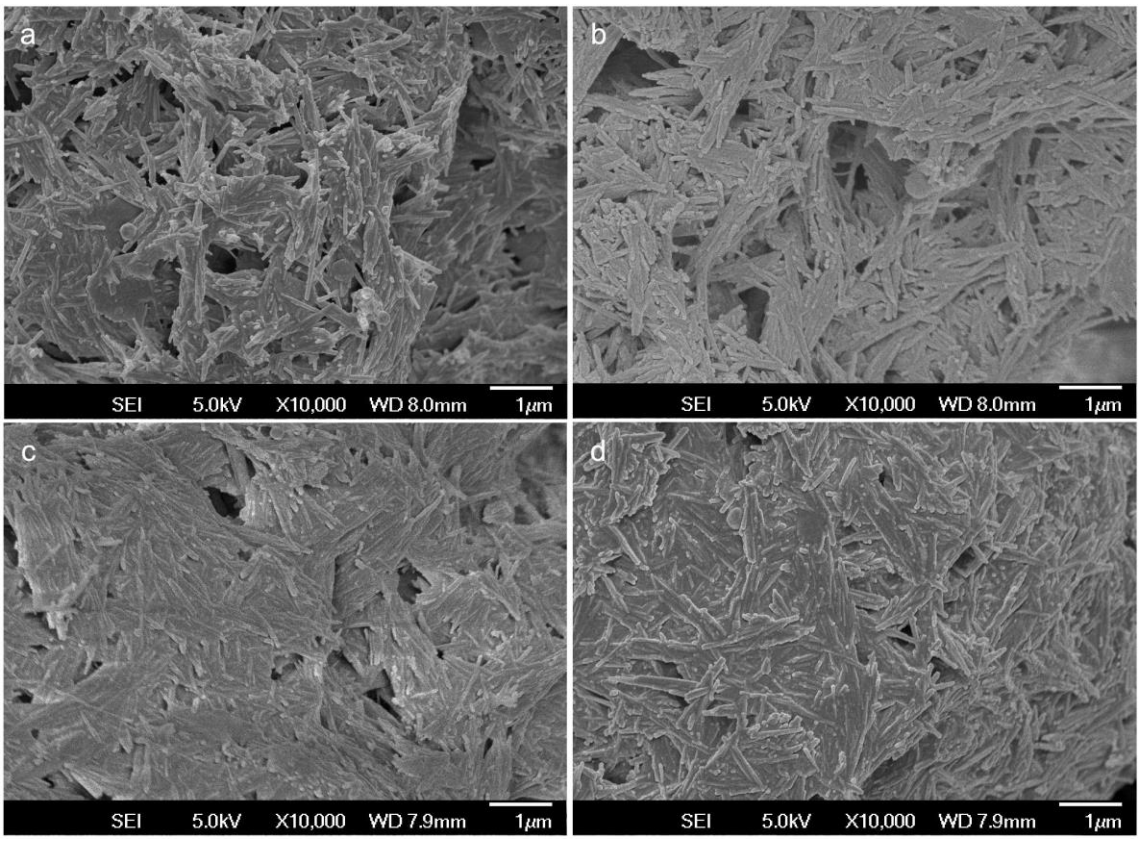

Fig. S13. SEM images of the PAL@fluoroPOS/PFDTES coatings with a $C_{PFDTES\text{-}ii}$ of (a) 0, (b) 5.7, (c) 11.3 and (d) 17.0 mM. C_{PAL} = 10 g L^{-1}, $C_{PFDTES\text{-}i}$ = 25 mM and C_{TEOS} = 4.5 mM.

Table S2. CAs and SAs of liquids droplets (5 μL) with different surface tension on the PAL@fluoroPOS/PFDTES coating at 25 ℃.

Liquids	CA / °	SA / °	Surface tension (mN m^{-1}, 20 ℃) [3]
water	165.6 ± 1.2	1.0 ± 0.0	72.8
glycerol	164.4 ± 0.2	1.0 ± 0.0	64.0
diiodomethane	163.3 ± 1.5	1.6 ± 0.6	50.8
N-methyl-2-pyrrolidone	162.1 ± 0.7	3.7 ± 0.6	40.8
toluene	159.2 ± 1.4	4.0 ± 0.0	28.4
n-hexadecane	159.1 ± 1.0	4.3 ± 0.7	27.5
n-dodecane	158.2 ± 0.7	6.7 ± 0.7	25.4
n-decane	156.0 ± 0.3	9.0 ± 1.0	23.8
n-octane	153.6 ± 1.0	18.3 ± 1.2	21.6

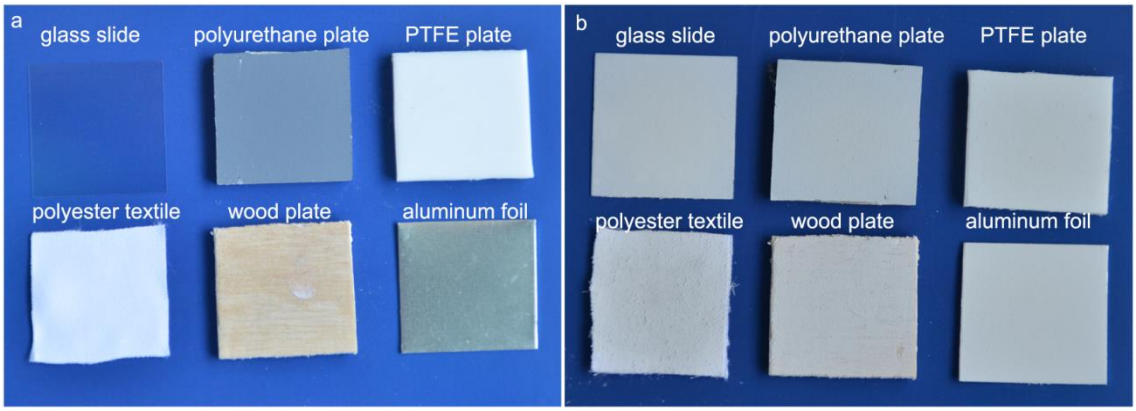

Fig. S14. Images of (a) different substrates and (b) the PAL@fluoroPOS/PFDTES coatings prepared on the corresponding substrates. C_{PAL} = 10 g L^{-1}, $C_{PFDTES\text{-}i}$ = 25 mM, C_{TEOS} = 4.5 mM and $C_{PFDTES\text{-}ii}$ = 11.3 mM.

Table S3. $CA_{n\text{-decane}}$ and $SA_{n\text{-decane}}$ of the PAL@fluoroPOS/PFDTES coatings prepared on different substrates. C_{PAL} = 10 g L^{-1}, $C_{PFDTES\text{-}i}$ = 25 mM, C_{TEOS} = 4.5 mM and $C_{PFDTES\text{-}ii}$ = 11.3 mM.

Substrates	$CA_{n\text{-decane}}$ / °	$SA_{n\text{-decane}}$ / °
glass slide	156.0 ±0.6	9.2 ±0.2
polyurethane plate	156.1 ±0.6	8.9 ±0.7
PTFE plate	156.3 ±0.6	9.8 ±0.4
polyester textile	156.3 ±0.7	9.6 ±0.4
wood plate	156.2 ±0.7	10.1 ±0.4
aluminum foil	156.2 ±0.9	8.1 ±0.9

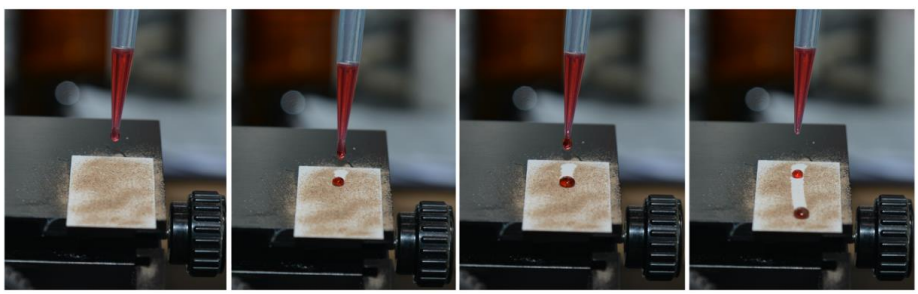

Fig. S15. Removal of sand microparticles on the surface of the PAL@fluoroPOS/PFDTES coating using *n*-decane. C_{PAL} = 10 g L^{-1}, $C_{PFDTES\text{-}i}$ = 25 mM, C_{TEOS} = 4.5 mM and $C_{PFDTES\text{-}ii}$ = 11.3 mM.

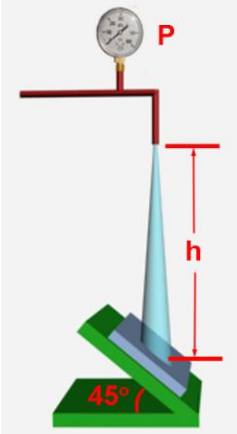

Fig. S16. Schematic illustration of the water jetting test.

For the water jetting tests, water jet at certain pressure scoured the 45 ° tilted surface from a height of 20 cm for a period of time.[4] The velocity (v, m s^{-1}) of water jetting on the sample surface was calculated as[5]

$$v = (\frac{2P}{\rho})^{1/2} \quad \text{(S1)}$$

Where P is the measured water pressure (kPa), ρ is water density (kg m^{-3}). When P is 25, 50, 100, 125 and 150 kPa, v is 7.1, 10.0, 14.1, 15.8 and 17.3 m s^{-1}, respectively.

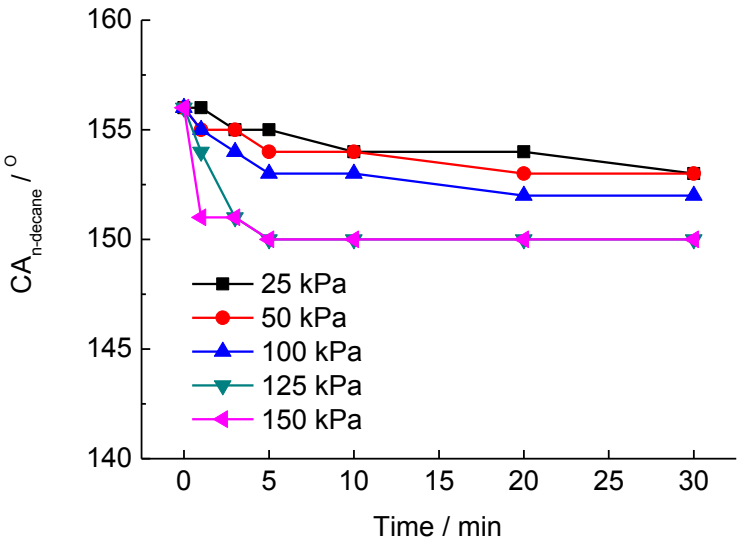

Fig. S17. Effect of water jetting pressure on $CA_{n\text{-decane}}$ of the PAL@fluoroPOS/PFDTES coating. C_{PAL} = 10 g L^{-1}, $C_{PFDTES\text{-}i}$ = 25 mM, C_{TEOS} = 4.5 mM and $C_{PFDTES\text{-}ii}$ = 11.3 mM.

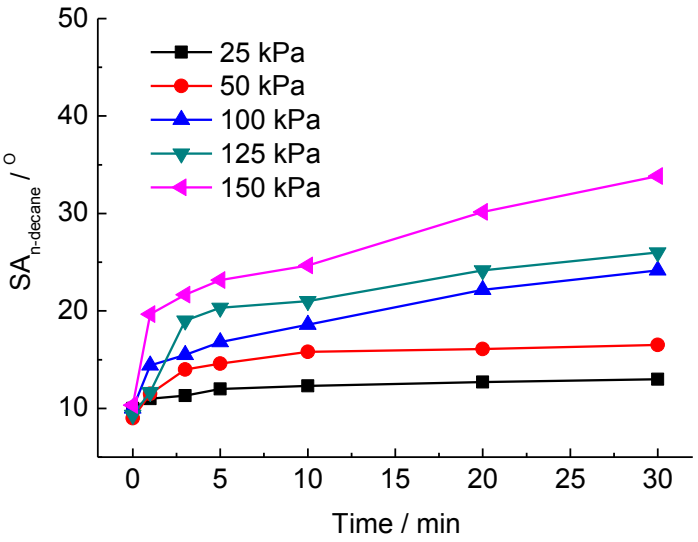

Fig. S18. Effect of water jetting pressure on $SA_{n\text{-decane}}$ of the PAL@fluoroPOS/PFDTES coating. C_{PAL} = 10 g L^{-1}, $C_{PFDTES\text{-}i}$ = 25 mM, C_{TEOS} = 4.5 mM and $C_{PFDTES\text{-}ii}$ = 11.3 mM.

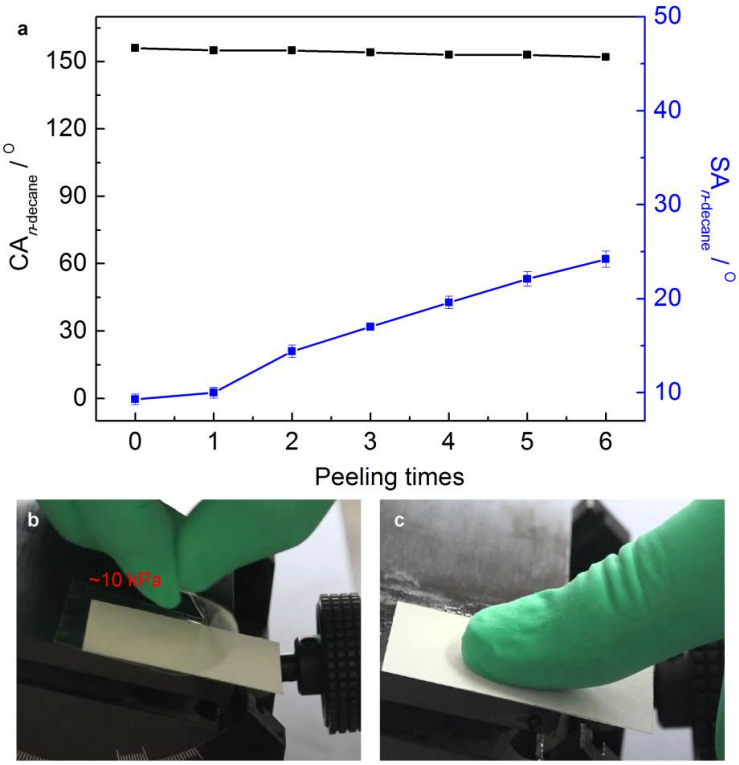

Fig. S19. (a) Changes of $CA_{n\text{-decane}}$ and $SA_{n\text{-decane}}$ of the PAL@fluoroPOS/PFDTES coating with peeling times using adhesive tape, qualitative tests of mechanical durability via (b) peeling with adhesive tape and (c) finger press. C_{PAL} = 10 g L^{-1}, $C_{PFDTES\text{-}i}$ = 25 mM, C_{TEOS} = 4.5 mM and $C_{PFDTES\text{-}ii}$ = 11.3 mM.

Table S4. $CA_{n\text{-decane}}$ and $SA_{n\text{-decane}}$ of the PAL@fluoroPOS/PFDTES coating after treated under various conditions. C_{PAL} = 10 g L^{-1}, $C_{PFDTES\text{-}i}$ = 25 mM, C_{TEOS} = 4.5 mM and $C_{PFDTES\text{-}ii}$ = 11.3 mM.

	$CA_{n\text{-decane}}$ / °	$SA_{n\text{-decane}}$ / °
after preparation	156.2 ± 1.0	9.2 ± 0.6
UV (200 W, 200-400 nm, 10 cm) , 1 h	156.0 ± 1.0	9.0 ± 0.6
liquid N_2, 1 h	156.6 ± 1.0	10.1 ± 0.7
350 ℃, 1 h	156.8 ± 1.0	11.8 ± 0.6
1 M $HCl_{(aq)}$, 1 h	155.3 ± 1.1	11.3 ± 0.6
1 M $NaOH_{(aq)}$, 1 h	155.7 ± 1.1	10.1 ± 0.7
saturated $NaOH_{(aq)}$ (~50 wt%), 1 h	155.2 ± 1.1	11.3 ± 1.2
saturated $NaCl_{(aq)}$ (~3.5 M), 1 h	155.0 ± 1.0	10.3 ± 1.1
98% H_2SO_4, 1 h	155.3 ± 1.1	17.5 ± 1.8
n-octane, 1 h	155.4 ± 1.0	10.6 ± 0.6
toluene, 1 h	155.6 ± 1.3	11.3 ± 1.6
boiling ethanol, 1 h	152.6 ± 1.3	20.2 ± 1.6
boiling water, 1 h	151.8 ± 1.5	24.5 ± 1.9
water, 240 h	155.4 ± 1.8	11.2 ± 0.3

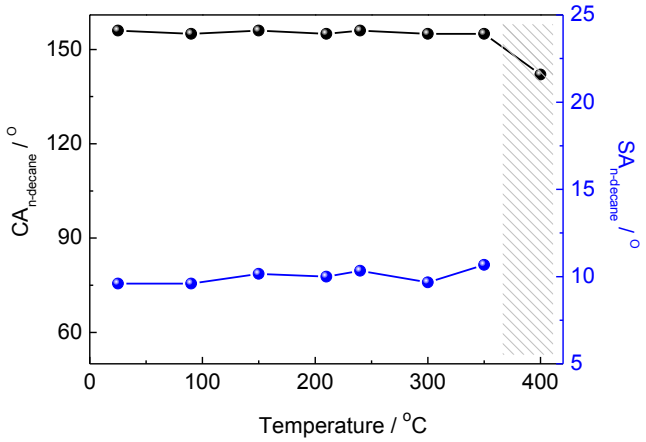

Fig. S20. Changes of $CA_{n\text{-decane}}$ and $SA_{n\text{-decane}}$ of the PAL@fluoroPOS/PFDTES coating after annealed at different temperature for 1 h. C_{PAL} = 10 g L^{-1}, $C_{PFDTES\text{-}i}$ = 25 mM, C_{TEOS} = 4.5 mM and $C_{PFDTES\text{-}ii}$ = 11.3 mM.

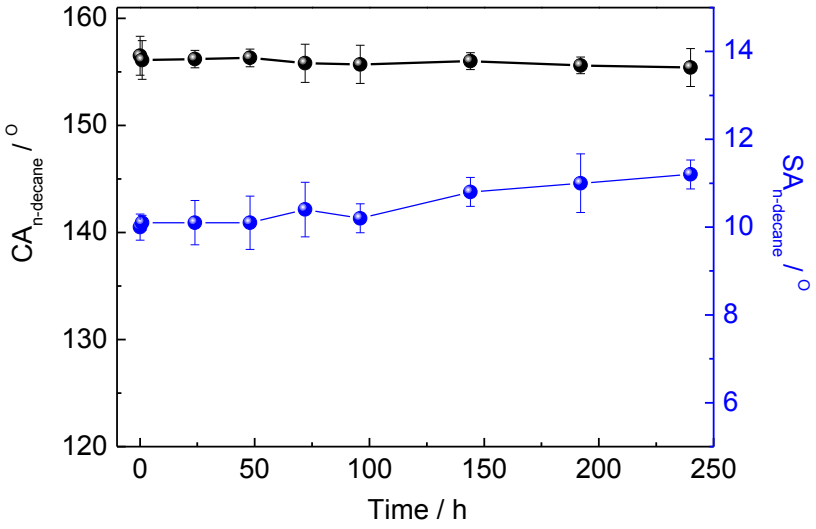

Fig. S21. Changes of $CA_{n\text{-decane}}$ and $SA_{n\text{-decane}}$ of the PAL@fluoroPOS/PFDTES coating after immersed in water for 240 h. C_{PAL} = 10 g L^{-1}, $C_{PFDTES\text{-}i}$ = 25 mM, C_{TEOS} = 4.5 mM and $C_{PFDTES\text{-}ii}$ = 11.3 mM.

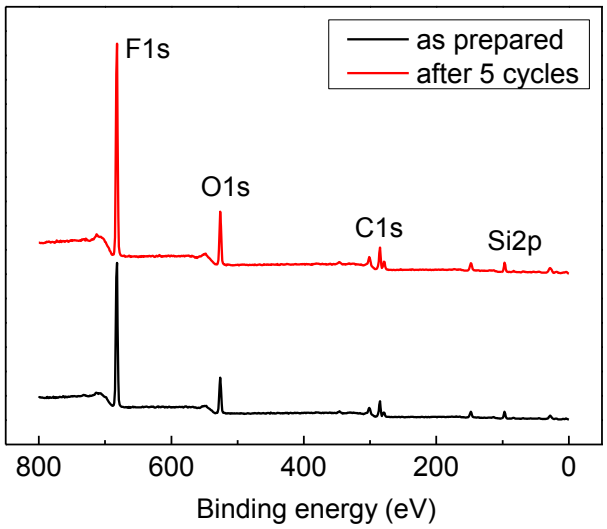

Fig. S22. XPS survey spectra of the as-prepared PAL@fluoroPOS/PFDTES coating and the coating after five plasma/self-healing cycles. C_{PAL} = 10 g L^{-1}, $C_{PFDTES\text{-}i}$ = 25 mM, C_{TEOS} = 4.5 mM and $C_{PFDTES\text{-}ii}$ = 11.3 mM.

Movie S1. Jets of 94 ℃ water and 70 ℃ *n*-hexadecane bounce off the PAL@fluoroPOS/PFDTES coating. This video demonstrates the excellent superamphiphobicity of the coating for hot liquids.

Movie S2. Water jetting test of the PAL@fluoroPOS/PFDTES coating at 100 kPa. This video highlights the excellent mechanical durability of the coating.

Movie S3. Boiling the PAL@fluoroPOS/PFDTES coating in water. This video demonstrates the high durability of the coating in hot liquids.

References

1. J. T. Han, S. Y. Kim, J. S. Woo and G. W. Lee, *Adv. Mater.*, 2008, **20**, 3724-3727.
2. A. Vilcnik, I. Jerman, A. Surca Vuk, M. Kozelj, B. Orel, B. Tomsic, B. Simoncic and J. Kovac, *Langmuir*, 2009, **25**, 5869-5880.
3. http://www.surface-tension.de.
4. B. Li and J. Zhang, *Carbon*, 2015, **93**, 648-658.
5. D. Ge, L. Yang, Y. Zhang, Y. Rahmawan and S. Yang, *Part. Part. Syst. Char.*, 2014, **31**, 763-770.